# Wideband Non-Reciprocal Magnetic-free Devices Based on High-Order Spatio-Temporal Modulation

Mahmoud Nafe, Xiaohu Wu, Xiaoguang Liu
Electrical and Computer Engineering Department
University of California Davis
Davis, 95616, CA, USA
Email: manafe@ucdavis.edu

***Abstract*—In this paper, we demonstrate that wideband non-reciprocal magnetic-free devices with flat and low loss in-band transmission, high isolation, and good matching at each ports, can be obtained by using higher-order spatio-temporal modulation (STM). As a proof-of-concept, a 3-pole filtering isolator at $200$ MHz and a 2-pole circulator at $450$ MHz are designed and tested. The filtering isolator demonstrates an insertion loss of $1.5$ dB with a suppressed reverse isolation better than $20$ dB across the frequency range of $170$–$203$ MHz. The circulator shows an insertion loss of $3.8$ dB with a reverse isolation better than $15$ dB across the frequency range of $400$–$470$ MHz.**

***Keywords*—Magnetic-free, Non-Reciprocity, Spatio-Temporal Modulation.**

## I. Introduction

Conventionally, non-reciprocity in the RF and microwave frequency ranges is achieved using ferromagnetic materials exposed to an external magnetic field. This approach results in devices, such as isolators and circulators, that are bulky, expensive, and hard to integrate with other circuitries. Angular momentum biasing was introduced in [1] as an alternative biasing technique that does not require a magnetic field. The non-reciprocity was achieved by spatio-temporal modulation (STM) of the relative permittivity of a ring resonator along the azimuth direction with a sinusoidal wave of frequency $f_m$. The modulation creates intermodulation products ($f_{RF} \pm f_m$) with a preferred sense of rotation, i.e. the degeneracy of the resonant modes are shifted by the application of the angular modulation. Conceptually, the modulation is taking place in space (modulating the medium) and by a time-varying signal, hence the name spatio-temporal modulation [2]. The disadvantage with this approach is a relatively weak modulation effect.

More efficient implementations were illustrated in [2]–[4], where instead of modulating a continuum medium, the ring resonator is broken up into 3 coupled resonators. Furthermore, STM was achieved by having a progressive phase shift of $120^\circ$ applied to the modulation signals. In [3], 3 series LC resonators were connected in a $Y$ topology. Although the circulator showed a directivity ($|S_{21}|$ (dB)-$|S_{31}|$ (dB)) better than $50$ dB, it suffered from a large insertion loss of approximately $10$ dB. The loss was attributed to the generation of a large number of higher order intermodulation (IM) products. In [4], a differential architecture was proposed to reduce the spurious IM products. The proposed architecture is comprised of two single-ended (SE) STM-based circulators with opposite rotation direction, i.e. there is a $180^\circ$ phase difference between the modulation signals applied to each SE circulator. When compared to the SE circulators, the differential architecture not only significantly improved the circulator performances in terms of insertion loss, return loss, and isolation, but also relaxed the required modulation frequency and amplitude.

To date, all reported STM-circulators utilize first order resonators as depicted in Fig. 1 (a). This leads to a narrow directivity bandwidth that in the range of 2–3% [2]–[4]. In [5], a directivity bandwidth of 13.9% was achieved by using a bandpass filter as a matching network between the RF ports and the circulator interface, while the circulator core is still first-order. In this work, we propose an alternative approach to widening the directivity bandwidth by incorporating a 2-pole bandpass resonators as shown in Fig. 1(b). Compared to [5], the proposed approach has the advantage of using less number of components. In addition, it adds degrees of freedom to the circulator design, because the modulation parameters

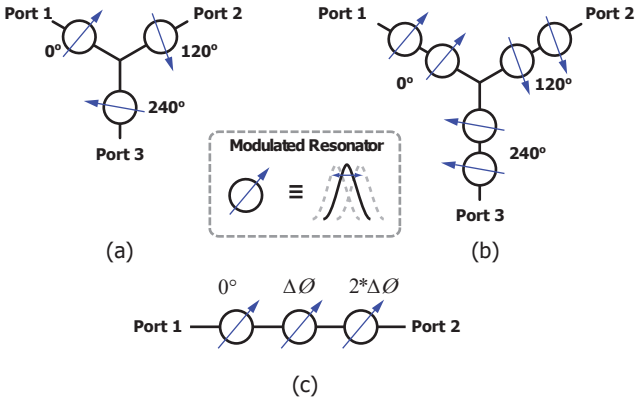


Fig. 1. Magnetic-free circulator based on STM of (a) resonators and (b) 2-pole bandpass filters, and (c) magnetic-free filtering isolator based on STM of 3-pole bandpass filter.

Approved for public release: distribution is unlimited. Approval ID: HR0011-17-C-0029.

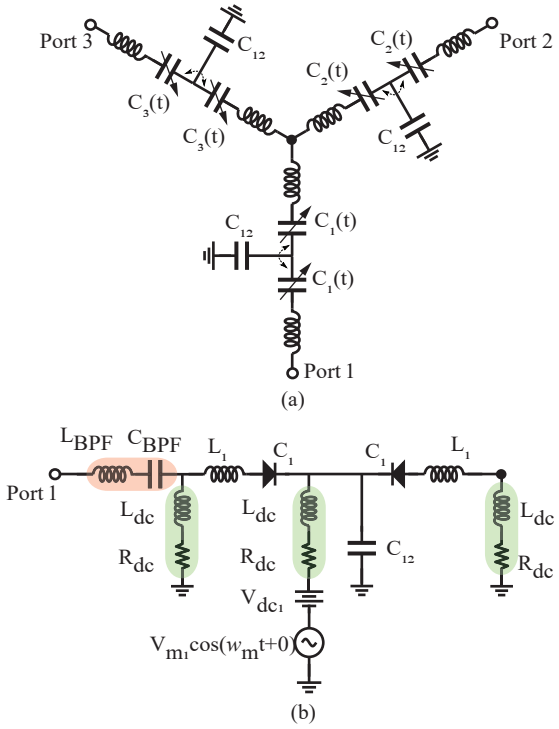


Fig. 2. Proposed circulator architecture: (a) 2-pole bandpass resonators connected in a $Y$ topology and (b) practical implementation of a time-varying capacitor using varactors along with the necessary biasing network and filters.

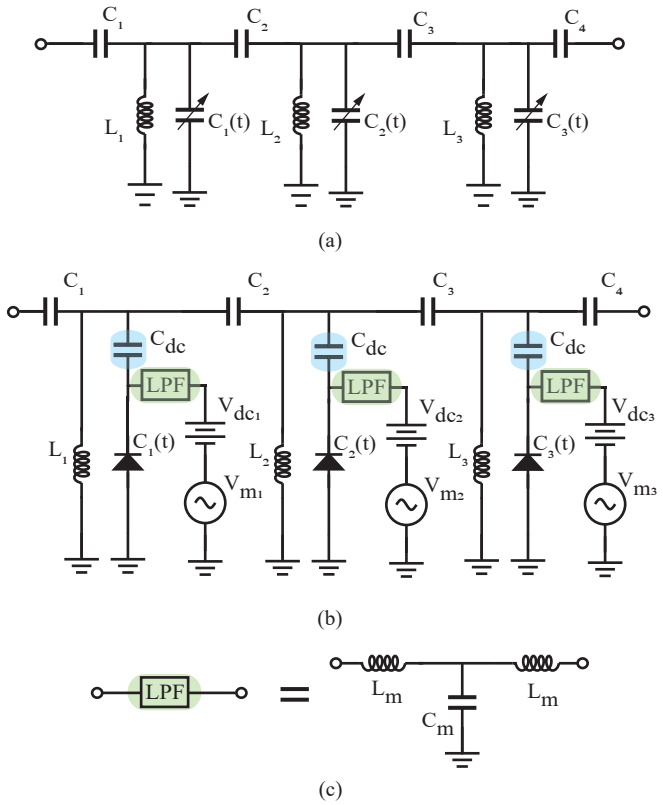


Fig. 3. (a) LC implementation of 3-pole non-reciprocal filter using ideal time-varying capacitors. (b) Practical circuit implementation of 3-pole non-reciprocal filter with varactors. (c) Bias LPF circuit.

of each resonator can be set separately. To further illustrate the effectiveness of the proposed widening technique, we also present a 2-port STM non-reciprocal filter that also functions as an isolator. In the same manner, the filtering isolator is based on higher order (third order) coupled resonators as shown in Fig.1 (c). In Section II, we discuss the design of both circuits. Second, section III demonstrates the measurement results. Finally, section III concludes and summarizes the paper.

## II. Proposed Non-Reciprocal Architecture

### A. Circulator

As shown in Fig. 2 (a), the proposed circulator is composed of three 2-pole bandpass (series LC resonators) filter connected in a $Y$ topology. The resonant frequency, i.e. the operation frequency of circulator, is chosen to be 500 MHz to ensure the availability of modulation sources and high quality factor passive components . The coupling between each resonator is controlled by a shunt capacitor $C_{12}$.

The STM of the filter center frequency is achieved by modulating the capacitance of each resonator. In practice, the variable capacitors are also implemented with diode varactors. For simplicity, the modulation phase of the two varactors in each filter branch is set to be the same. Similar to Fig. 1, there is a progressive phase shift of 120° between the three filter branches in order to implement angular momentum biasing.

Fig. 2 (b) depicts a practical implementation of the STM using diode varactors along with the necessary biasing networks.

The overall capacitance of the varactors can be expressed mathematically as

$$C_n(t) = C_0 + \Delta C \cos\left[\omega_m t + \frac{2(n-1)\pi}{3}\right], \qquad (1)$$

where $n = 1, 2, 3$, $C_0$ is the mean capacitance when the varactors are biased with dc voltage $V_{dc}$, $\Delta C$ is the modulation index that relates to $V_m$, and $\omega_m$ is the modulation frequency. Furthermore, a bandpass filter ($L_{BPF}$ and $C_{BPF}$) with center frequency at $f_{RF}$ is used to eliminate any interference between the input RF frequency ($f_{RF}$) and the modulation frequency ($f_m$). Finally, a low pass filter ($L_{dc}$) in series with a resistor ($R_{dc}$) are used to provide a path to ground for the dc bias and the modulation frequency.

### B. Filtering isolator

Fig. 3 (a) shows the 3-pole LC implementation of filtering integrated isolator. $C_1$ and $C_4$ serve as the coupling between the resonators and source/load, and $C_2$ and $C_3$ are the coupling between resonators. The center frequency of the three parallel resonators are modulated with a progressive phase shift of $\Delta\phi$

$$C_n(t) = C_n + \Delta C \cos\left[\omega_m t + (n-1)\Delta\phi\right], \qquad (2)$$

where $n = 1, 2, 3$, $C_n$ is the mean capacitance without modulation, $\Delta C$ is the modulation index, $\omega_m$ is the modulation

frequency, and $\Delta\phi$ is the modulation phase shift between adjacent resonators.

As shown in Fig. 3 (b), the ideal time-varying capacitors in (Fig. 3 (a)) are implemented by reverse-biased varactor diodes. To provide the modulation voltage on the varactors, a dc-blocking capacitor $C_{dc}$ is connected in series with the varactor to isolate the shunt inductor from the dc path. The series coupling capacitors also serve to isolate the modulation signal $f_m$ from leakage to RF ports. A bias voltage $V_{dc}$ is provided to each varactor to set the nominal capacitance value. A modulation voltage $V_m$ is provided to each varactor with a constant phase shift $\Delta\phi$ between the varactors. $V_m$ is provided through a low-pass filter (LPF) to isolate $f_m$ from $f_0$. The third-order LPF circuit is shown in Fig. 3 (c).

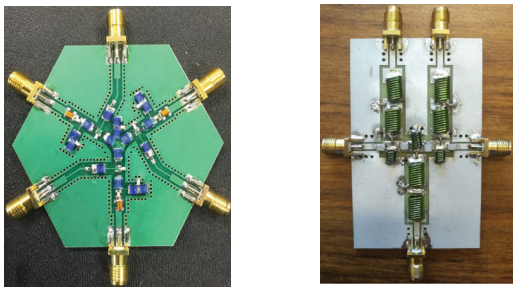

(a) (b)

Fig. 4. (a) Fabricated magnetic-free circulator and (b) filtering isolator.

## III. Results and Discussion

The physical design of both circuits is carried out on a 62-mil FR-4 substrate. The dielectric loss of the FR-4 substrate is not a significant concern in this design due to the relatively low center frequency. Realistic models from the component vendors are used to simulate and optimize the circuit performance. The optimized component values for the circulator are $L_1 = 120\,\text{nH}$, $L_{BPF} = 27\,\text{nH}$, $L_{DC} = 180\,\text{nH}$, $C_{BPF} = 3.9\,\text{pF}$, $C_{12} = 5.6\,\text{pF}$, $V_{dc} = 4.4\,\text{V}$, $V_m = 2.2\,\text{V}$, $f_m = 60\,\text{MHz}$. Similarity, those for the filtering isolator are $L_1 = L_3 = 47\,\text{nH}$, $L_2 = 68\,\text{nH}$, $C_{dc} = 82\,\text{pF}$, $C_1 = C_4 = 8.2\,\text{pF}$, $C_2 = C_3 = 2.4\,\text{pF}$, $L_m = 180\,\text{nH}$, $C_m = 82\,\text{pF}$, $f_m = 30\,\text{MHz}$, $\Delta\phi = 70°$. Fig. 4 (a) and (b) show the pictures of the fabricated magnetic-free isolator and circulator, respectively. The circulator over all area is $6.7 \times 5.9\,\text{cm}^2$, while that of the isolating filter is $8 \times 4.5\,\text{cm}^2$.

Fig. 5 shows the simulated and measured results of the presented 2-pole circulator. When there is no modulation, i.e. the varactors are only reverse-biased with dc voltage of 5.5 V, as shown in Fig. 5 (a), the circuit is reciprocal with an in-band insertion loss 3.5 dB due to the equal power splitting along the $Y$ branches. By applying a sinusoidal signal with modulation frequency of 74 MHz and amplitude of 1.3 V, the non-reciprocal responses shown in Fig. 5 (b)–(d) are obtained. It is worth mentioning that Skyworks SMV1231 varactor has been used. The 2-pole filter based circulator shows a flatter passband (Fig. 5 (b)), return loss better than 10 dB (Fig. 5 (d)),

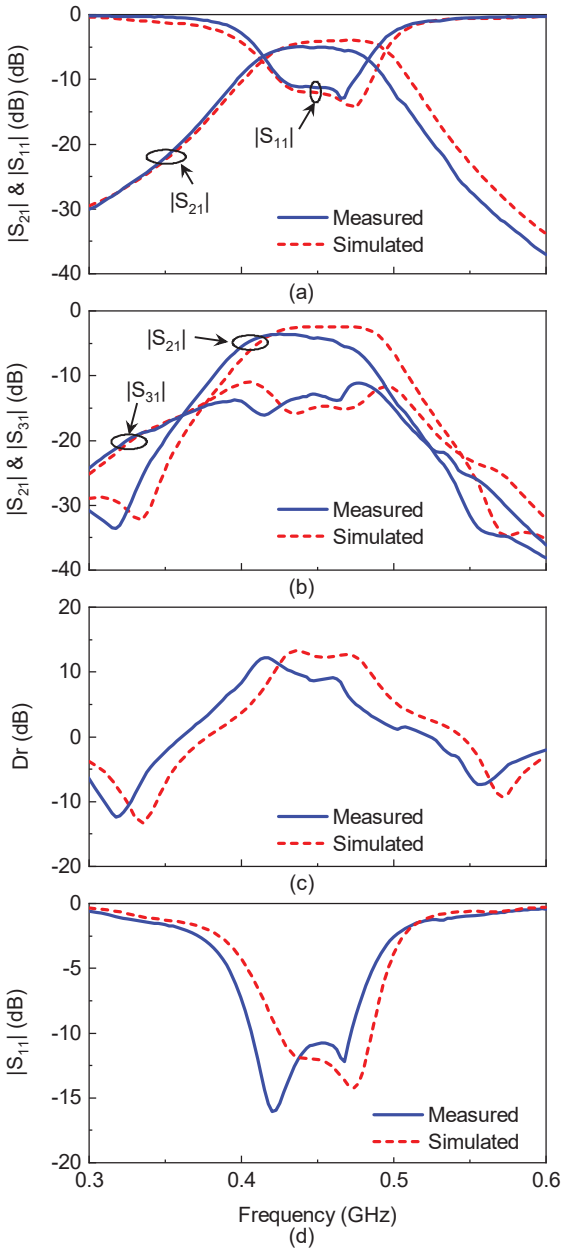


Fig. 5. Simulated and measured S-parameters of the proposed 2-pole circulator: (a) Non-modulated responses. (b) Modulated $|S_{21}|$ and isolation $|S_{31}|$. (c) Directivity $D_r$. (d) Port reflection $|S_{11}|$.

and an $D_r$ with dual absolute poles over a wide frequency range (Fig. 5 (c)). All the simulated and measured results are well agreed and validate the effectiveness of the presented high-order STM technology.

Fig. 6 (a) shows the simulated and measured S-parameters of the filtering isolator when there is no spatio-temporal modulation. The reverse-biased dc voltage on the three varactors are 5.0 V, 4.7 V, and 5.0 V, which give an equivalent static capacitance of 6 pF, 6.3 pF, and 6.0 pF, respectively. The static filter exhibits an equal-ripple bandwidth of 29 MHz, a 3-dB bandwidth of 45 MHz (175–220 MHz), and a minimum

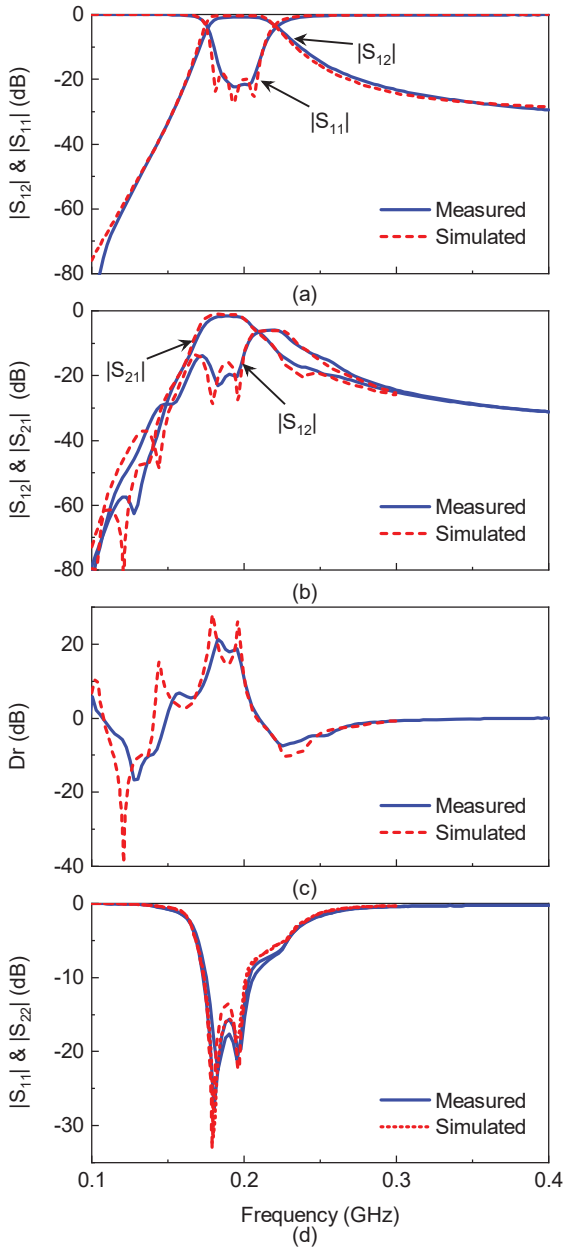


Fig. 6. Simulated and measured S-parameters of the proposed filtering isolator: (a) Non-modulated responses. (b) Modulated transmission $|S_{21}|$ and reverse isolation $|S_{12}|$. (c) Directivity of the isolator. (d) Port reflection $|S_{11}|$ and $S_{22}$.

insertion loss of 0.8 dB. The measurement agrees very well with the simulation.

Fig. 6 (b)–(d) shows the filter responses under spatio-temporal modulation, where the modulation frequency $f_m$ is set to 28 MHz. Moreover, the modulation voltages applied across the varactors are 2.4 V, 2.3 V, and 2.4 V, corresponding to capacitance variation of 5.0–10 pF. The optimal modulation phase difference $\Delta\phi$ between the adjacent sources is found to be 70°. Fig. 6 (b) shows the measured $|S_{21}|$ and $|S_{12}|$ in comparison with the the simulation. The filter has a very good forward filtering response with a minimum passband insertion loss of 1 dB in simulation and 1.5 dB in measurement. The measured 3-dB bandwidth covers the frequency range of 170–203 MHz which is slightly smaller than the non-modulated case. Reverse isolation $|S_{12}|$ of the filter has two zeros in the filter's passband, resulting in an $D_r$ of better than 20 dB in the passband (Fig. 6 (c)). The filter is well matched at both ports showing better than 15 dB of return loss.

## Conclusions

In this paper, high-order spatio-temporal modulation is developed to obtain wideband non-reciprocity with flat passband transmission and high reverse isolation. The proposed magnetic-less non-reciprocal devices with its large isolation bandwidth along with the flat passband responses makes it a suitable candidate for applications such as full duplex wireless communication, frequency division relay systems, and automotive radars.

## Acknowledgment

This research is funded by the Defense Advanced Research Projects Agency (DARPA) under the Signal Processing at RF (SPAR) program (Contract #: HR0011-17-C-0029).

## References

[1] D. L. Sounas, C. Caloz, and A. Alu, "Giant non-reciprocity at the subwavelength scale using angular momentum-biased metamaterials," Nat. Commun., vol. 4, p. 2407, Sept. 2013.

[2] N. A. Estep, et al. "Magnetic-free non-reciprocity and isolation based on parametrically modulated coupled-resonator loops," Nature Physics, vol. 10, no. 12, pp. 923-927, 2014.

[3] N. A. Estep, D. L. Sounas, and A. Alu, "Magnetless microwave circulators based on spatiotemporally modulated rings of coupled resonators," IEEE Trans. Microw. Theory Techn., vol. 64, no. 2, pp. 502-518, 2016.

[4] Ahmed Kord, Dimitrios L. Sounas, Andrea Alu, "Pseudo-Linear Time-Invariant Magnetless Circulators Based on Differential Spatiotemporal Modulation of Resonant Junctions," IEEE Trans. Microw. Theory Techn., vol. 66, no. 6, pp. 2731-2745, 2018

[5] Ahmed Kord, Dimitrios L. Sounas, Zhicheng Xiao, Andrea Alu, "Broadband Cyclic-Symmetric Magnet-less Circulators and Theoretical Bounds on their Bandwidth," arXiv:1805.0194.